Contents lists available at SciVerse ScienceDirect

Physica B

Current-conduction mechanisms in Au/*n*-CdTe Schottky solar cells in the wide temperature range

Songül Fiat [a,*], Ziya Merdan [b], Tofig Memmedli [b,c]

[a] Physics Department, Faculty of Arts and Sciences, Gaziosmanpaşa University, 60240 Tokat, Turkey
[b] Physics Department, Faculty of Arts and Sciences, Gazi University, 06500 Ankara, Turkey
[c] National Academy of Science, Institute of Physics, Baku, Azerbaijan

ARTICLE INFO

ABSTRACT

The current-conduction mechanisms in Au/*n*-CdTe Schottky solar cells have been investigated by considering the series resistance (R_s) effect in the temperature range 120–380 K. The obtained values of main electrical parameters such as zero-bias barrier height (Φ_{bo}), ideality factor (n) and R_s were found strongly function of temperature. While the Φ_{bo} increases, the n decreases with the increasing temperature. Such behavior can be explained on the basis of the thermionic emission (TE) theory with the Gaussian distribution (GD) of the barrier height (BH) being related to inhomogeneities at the metal/semiconductor (M/S) interface. The results show that the conduction mechanism in Au/*n*-CdTe Schottky solar cells can be successfully explained on the basis of the TE mechanism with a GD of the BHs. In addition, the capacitance–voltage (*C–V*) characteristics of Au/*n*-CdTe solar cells have been investigated at room temperature and 1 MHz.

1. Introduction

The analysis of the current–voltage (*I–V*) characteristics in metal–semiconductor (MS) contacts and solar cells under dark or illumination is a very important issue especially at low temperatures. It is well known that only at room or a narrow temperature range does not give a detailed information about their conduction mechanisms and the nature of barrier height formation at M/S interface. On the other hand, the *I–V* characteristics at a wide temperature range can allow us to understand different aspects of conduction mechanism or the nature of barrier formation. In order to find which current-conduction mechanism is dominate in the certain temperature and applied bias voltage region, the *I–V* characteristics of these devices at a wide temperature range must be taken into consideration. Because, there are a great number of carrier/current-conduction/transport mechanisms such as thermionic emission (TE), thermionic field emission (TFE), field emission (FE), minority carrier injection, recombination–generation, tunneling via interface states or dislocations and multistep tunneling [1,2]. However, simultaneous contribution from two or more mechanisms could also be possible in the certain temperature and voltage ranges.

Cadmium telluride (CdTe) has gained considerable interest as one of the most promising II–VI semiconductors, and there has been an active interest in CdTe due to its direct band gap of $\sim$1.45 eV, large absorption coefficient, and reasonable mobility-lifetime product for both electrons and holes. A comprehensive understanding of the basics of CdTe is needed for improvements to be achieved. Electroluminescence (EL) and photoluminescence (PL) were the primary techniques developed for this purpose. In EL, forward-bias is used to inject excess carriers. With PL, excitation of excess carriers is provided by a laser [3]. Although CdTe thin films can be prepared by various techniques, such as thermal evaporation, metal organic chemical vapor deposition, molecular beam epitaxy, sputtering and electrodeposition, electrodeposition is the simplest and the most economical method for large area solar cell applications [4,5]. In addition, there are many studies about metal/CdTe contacts, sensors in thermal imaging, solar cells etc. [6,7]. The dominant charge transport mechanisms in Au/CdTe devices have been identified as thermionic emission over the barrier, Poole–Frenkel, and space charge limited conduction [4–6]. Also, Pattabi et al. [3] have reported that the dominant current-conduction mechanism in the forward bias region seems to be thermionic emission–diffusion.

The analysis of current–voltage (*I–V*) characteristics of MS contacts which are known as Schottky barrier diodes (SBDs) and solar cells based on thermionic emission theory usually reveal an abnormal decrease in the barrier height Φ_{bo} and an increase in the

---

* Corresponding author. Tel.: +90 356 252 15 82; fax: +90 356 252 15 85.
  E-mail address: songulfiat@yahoo.com (S. Fiat).

identity factor n with decreasing temperature. The decrease in the barrier height at low temperatures leads to non-linearity in the activation energy $\ln(I_0/T^2)$ vs $1/T$ plot. Lately, the nature and origin of the temperature dependence of barrier height and the ideality factor have been successfully explained on the basis of the thermionic emission mechanism with the Gaussian distribution (GD) of the barrier heights (BHs) due to the inhomogeneities of the BHs at the M/S interface. In general, there are two main approaches to describe inhomogeneous SBHs. These approaches are proposed by Tung and by Werner and Gütter who assume a GD of the BH values at the M/S interface [8,9]. Tung's explanation for this phenomenon is a homogeneous formation as a distribution of patches with different low BH values and areas embedded within uniform higher Schottky barrier area [8]. Spatial inhomogeneity of the SBH at the M/S interface has been thoroughly discussed, and many electrical anomalies observed in the SBDs, such as the dependence of SBH on the measurement method, the temperature-dependence of the ideality factor, and a curved activation-energy plot etc., can be explained by assuming a GD of the SBH [9–11]. Simulation studies on the I–V characteristics of inhomogeneous diodes with a GD of BH have also yielded results similar to those observed in experiments [12–14]. Recently, the nature and origin of the decrease in the BH and increase in ideality factor with a concurrent decrease in temperature was reported in literature [8–15].

There are many studies about current-conduction mechanisms of such structures; but, the complete description of the current-conduction mechanisms of these devices has not been clarified in detail. Therefore, we can say that the temperature effect on the current-conduction mechanisms in Schottky solar cells is very important rather than its efficiency. Therefore, the I–V characteristics of the fabricated Au/n-CdTe of Schottky solar cells have been investigated in the wide temperature range by considering the R_s effect and the applied bias voltage. Experimental results show that the forward-bias I–V data reveals that an increase in the Φ_{bo} but a decrease in n with the increasing temperature. Such a temperature dependence is an obvious disagreement with the reported negative temperature coefficient of the BH or forbidden band gap (E_g) of a semiconductor. The decrease in Φ_{bo} and increase in n with the decreasing temperature have been interpreted on the basis of the TE theory with a spatial GD of the BHs around a mean value BH at the Au/n-CdTe interface.

2. Experiment details

For the fabrication process, an n-CdTe obtained with Bridgeman method, with (1 1 1) orientation and 500 μm thickness, was degreased in the organic solvents (CHClCCl$_2$), CH$_3$COCH, and CH$_3$OH consecutively; etched in a sequence of H$_2$SO$_4$ and H$_2$O$_2$, 20% HF a solution of (6HNO$_3$:1HF:35H$_2$O), and 20% HF; and finally, rinsed in de-ionized water for a prolonged time. Preceding each cleaning step, the wafer was rinsed thoroughly in de-ionized water of resistivity 18 M Ω cm. Immediately after surface cleaning, high-purity gold (Au) metal (99.999%) layer with a thickness of ~2000 Å was thermally evaporated onto the whole back surface of the CdTe wafer under a pressure of ~10^{-8} mbar in the turbo molecular vacuum-coating system (Bestek Technique). In order to form ohmic contacts on the back surface of the CdTe wafer, the wafer was annealed at 500 °C for 5 min in the same vacuum system. Following the formation of ohmic contact, circular dot layers with the area of 0.071 cm^2 and thickness of 1100 Å were deposited onto the front surface of the CdTe in order to form Au-rectifying contacts.

The current–voltage (I–V) measurements of Au/n-CdTe device was carried out using a Keithley 2400 Sourcemeter in the

temperature range 120–380 K using a temperature-controlled vpf-475 cryostat, which enables measurements in the temperature range 77–450 K. The bias voltage is swept from –6 to +6 V with 20 mV steps. The sample temperature was always monitored using a thermocouple close to the sample and measured with Keithley model 199 DMM/scanner and Lake Shore model 321 autotuning temperature controllers, with sensitivity better than $\pm$ 0.1 K. In addition, the capacitance–voltage (C–V) measurements were conducted using an HP 4192 A LF impedance analyzer at room temperature and 1 MHz. All measurements were carried out with the help of a microcomputer through an IEEE-488 ac/dc converter card.

3. Results and discussion

For a SBD, current transport is due to the majority carriers, and it may be described by TE over the interface barrier. The TE current at the forward bias can be written as [16–22]

$$I = I_0 \exp\left(\frac{q(V-IR_s)}{nkT}\right)\left\{1 - \exp\left(-\frac{q(V-IR_s)}{kT}\right)\right\}, \tag{1}$$

where q is the electronic charge, V is the applied voltage across the diode, k is the Boltzmann constant, T is the absolute temperature in K, R_s is the series resistance of the diode, IR_s term is the voltage drop across the R_s, n is the ideality factor, and I_0 is the reverse saturation current derived from the linear region of the intercept of $\ln I$–V at zero bias and can be expressed as

$$I_0 = AA*T^2\exp\left(-\frac{q\Phi_{bo}}{kT}\right), \tag{2}$$

where A is the rectifier contact area of the diode, A^* is the effective Richardson constant (12 A cm^{-2} K^{-2} for n-type CdTe) [2], and Φ_{bo} is the zero-bias BH of the diode. The value of Φ_{bo} is calculated from Eq. (2) for each temperature. The value of n is derived from the slope of the linear region of the forward-bias $\ln I$–V plot for each temperature and can be written as follows:

$$n = \frac{q}{kT}\left(\frac{dV}{d\ln I}\right). \tag{3}$$

In Fig. 1, the forward and reverse bias semi-logarithmic $\ln I$–V characteristics are shown. From these fits, the experimental values of n and Φ_{bo} were determined from the forward-bias $\ln I$–V plot at each temperature. Once I_0 is known, the zero-bias BH can be computed using Eq. (2). The Φ_{bo} and n determined from the semi-logarithmic forward I–V plots were found to be strong functions of temperature. It can be seen that the current rises slowly with applied reverse bias especially at low temperatures and does not show any effect of saturation. Such behavior of reverse bias current can be commonly explained in terms of barrier lowering or the barrier height (BH) is dependent of the electric field strength in the barrier as a result of the existence of an interfacial layer at metal/semiconductor interface. The lack of saturation current in reverse bias region can also be caused by image force lowering of the BH and due to the generation of electrons or holes in the depletion region as generation current is more pronounced at low temperatures than high temperatures [21]. Since the electric field strength increases with reverse bias, it follows that the BH decreases with an increase in the reverse bias. Because of the potential drop across the interfacial layer, the zero-bias barrier height (Φ_{bo}) is lower than the expected in an ideal diode, and similarly the potential across the interfacial layer varies with applied bias because of the electric field present in the semiconductor and the change in the interface state charges as a result of the applied bias voltage, and thus modifies the BH [18–22].
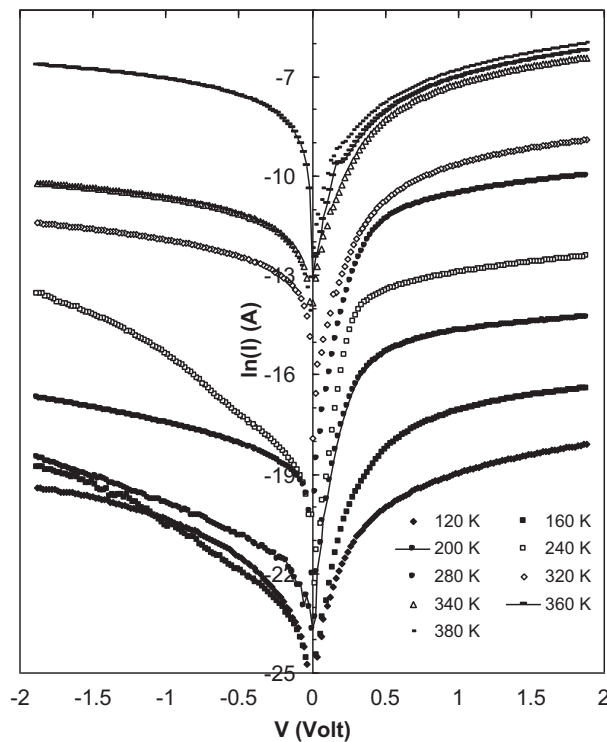
Fig. 1. Experimental forward and reverse bias *I–V* characteristics of the Au/*n*-CdTe Schottky solar cell at various temperatures.

Table 1
Temperature-dependent values of various parameters determined from the forward and reverse bias *I–V* characteristics of the Au/*n*-CdTe schottky solar cell.

T (K)	*n*	Φ_{bo} (eV)	I_0 (A)	R_s (at 2 V)(kΩ)
120	3.05	0.35	2.39E−11	8210
160	2.33	0.49	9.79E−12	2180
200	1.90	0.58	1.06E−10	298
240	1.62	0.68	2.64E−10	35.2
280	1.60	0.73	4.82E−09	3.8
320	1.57	0.78	5.04E−08	1.13
340	1.55	0.74	1.19E−06	0.0794
360	1.44	0.77	1.94E−06	0.056
380	1.44	0.78	5.76E−06	0.055

The experimental values of Φ_{bo} and *n* for the Au/*n*-CdTe Schottky solar cell was determined from Eqs. (2) and (3), respectively, and are reported in Table 1 and shown in Fig. 2. As reported in Table 1, the values of Φ_{bo} and *n* for the Au/*n*-CdTe structure ranged from 0.35 and 3.05 eV (at 120 K) to 0.78 and 1.44 eV (at 380 K), respectively. As the temperature increases, more and more electrons possess sufficient energy to surmount the higher barrier. As a result, the dominant BH will increase with the temperature and applied bias voltage. The greater-than-unity ideality factors are attributed to secondary mechanisms at the interface [17,18]. As explained in the reports by Gümüş et al. [19] and Tung [20], because current transport across the M/S interface is a temperature-activated process, electrons at low temperatures are able to surmount the lower barriers and therefore the current transport is dominated by current flowing through patches of the lower Schottky BH and hence leads to a larger ideality factor. As can be seen in Fig. 1, the semi logarithmic ln *I–V* plots are linear in the intermediate bias region ($0 \leq V \leq 0.7$); however, they deviate considerably from linearity because of series resistance in the high-voltage region ($V \geq 1.5$ V). On the other hand the dark
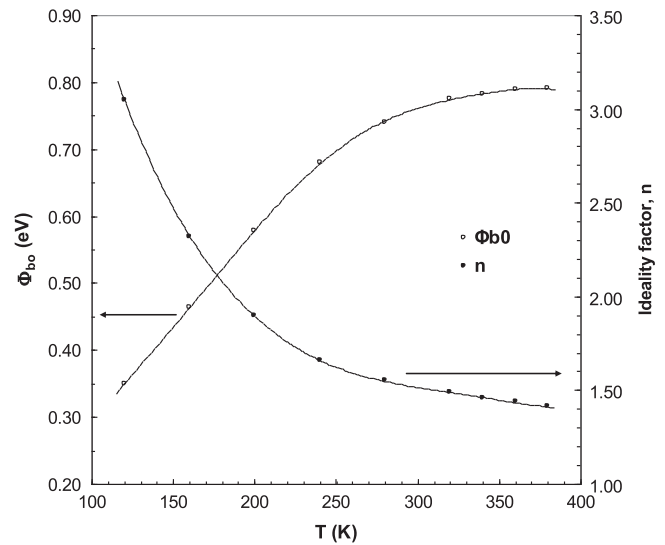

Fig. 2. Φ_{bo} vs *T* and ideality factor, *n* vs *T* curves of the Au/*n*-CdTe Schottky solar cell.

reverse current increases with the increasing applied reverse bias, and there is no mark due to the effect of saturation. As Table 1 shows, the values of the ideality factor are higher than unity for each temperature and increase with the decreasing temperature. The high values of the ideality factor show that there is a deviation from the TE theory in the current-transport mechanism, especially at lower temperature values ($T \leq 200$ K).

The series resistance effect on the electrical characteristics of the Au/CdTe Schottky solar cell was also investigated in the same temperature range. Because of the series resistance (R_s) is a very important parameter effect on Schottky diode characteristics. The resistance of the Schottky diode is the sum total resistance value of the resistors in series and resistance in semiconductor device in the direction of current flow. Therefore, the values of R_s are determined from the *I–V* curves at sufficiently high forward bias (2 V) for each temperature by using Ohm's Law ($\delta V/\delta I$) and are given in Table 1. As can be seen in Table 1, the value of R_s decreases with increasing temperature and varied from 8210 kΩ (at 120 K) to 55 Ω (at 380 K).

For the evaluation of the BH, Φ_{bo}, one may also make use of the activation energy (Richardson) plot of the saturation current. Eq. (4) can be rewritten as

$$\ln\left(\frac{I_0}{T^2}\right) = \ln(AA^*) - \frac{q\,\Phi_{bo}}{kT} \qquad (4)$$

As observed in Fig. 3, the dependence of $\ln(I_0/T^2)$ on q/kT is found to be linear in the temperature range of 200–380 K, but it deviates from linearity at low temperatures ($T \leq 200$ K). The experimental data asymptotically fit to a straight line (linear region) at high temperatures. The activation energy ($E_a = \Phi_{bo}$) and the Richardson constant (A^*) values were obtained from the slope and intercept at an ordinate of this linear region of the $\ln(I_0/T^2)$ vs q/kT plot as 0.52 eV and 4.06×10^{-3} A cm^{-2} K^{-2}, respectively, for the Au/*n*-CdTe solar cell. This value of A^* is much lower than the known value of 12 A cm^{-2} K^{-2} for the electrons of *n*-CdTe. The deviation in the Richardson plot may be due to the spatially inhomogeneous BHs and the potential fluctuations at the interface which consists of low and high-barrier areas; in other words, the current through the device will flow preferentially through the lower barriers in the potential distribution. However, the dependence of $\ln(I_0/T^2)$ vs q/nkT yields a straight line (Fig. 3). The values of E_a and A^* were obtained from the slope and intercept at an ordinate of the linear region of the
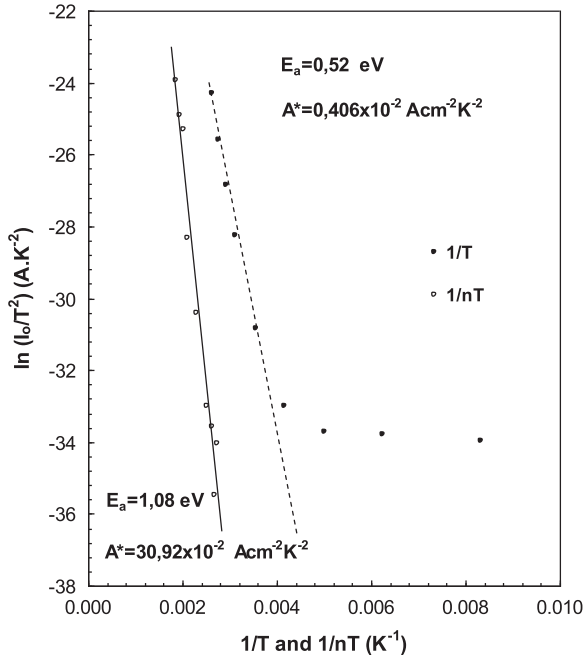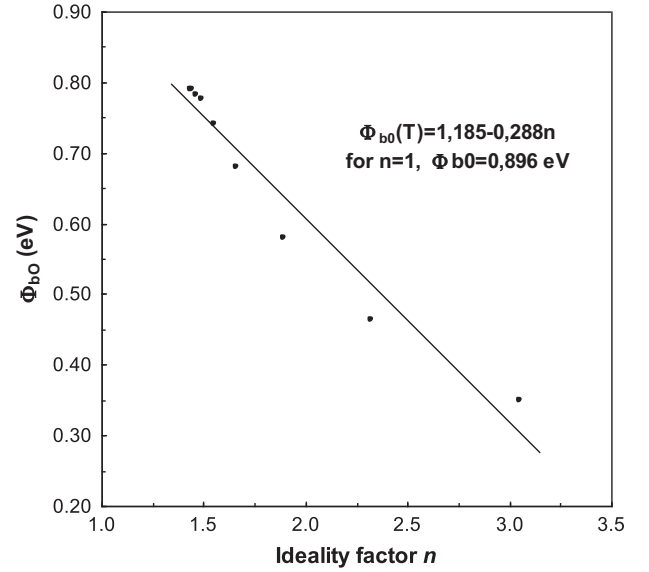
Fig. 3. Activation energy plot of $\ln(I_0/T^2)$ vs $1/T$ and $1/nT$ for the Au/n-CdTe Schottky solar cell.

Fig. 4. Φ_{bo} vs n for the Au/n-CdTe Schottky solar cell at various temperatures.

$\ln(I_0/T^2)$ vs q/nkT plot as 1.08 eV and 30.92 A cm^{-2} K^{-2}, respectively. This value of E_a is closer to the known value of 1.48 eV of the energy band gap of CdTe; nevertheless, the value of 30.92 A cm^{-2} K^{-2} is 2.08 times larger than the known value of 12 A cm^{-2} K^{-2} for the electrons of n-CdTe.

In general, the electrical characteristics of these devices do not obey the ideal Schottky theory. Usually, the thermionic emission (TE) mechanism is used to extract the main diode parameters [16] and the value of the ideality factor (n) is expected to be close to unity. However, a temperature-dependent analysis of the current–voltage (I–V) data reveals such an unusual behavior that the zero-bias barrier height (BH) decreases as the n value increases with decreasing temperature, and these changes are more pronounced particularly at low temperatures [16–18]. The decrease in the BH at low temperatures leads to nonlinearity in the activation energy plot of $\ln(I_0/T^2)$ vs $1/T$. Such behavior of the activation energy plot of Schottky solar cell at low temperatures has been attributed to the spatial variation in BHs. As explained above, the deviation in the Richardson plots might be a result of the spatially inhomogeneous BHs and potential fluctuations at the interface, which consist of low and high barrier areas [16–21]; in other words, the current through the barrier will flow preferentially through the lower barriers in the potential distributions. According to some authors [8–12,21–24], the ideality factor of an inhomogeneous solar cell with a distribution of low SBHs may increase with the decreasing temperature. Schmitsdorf et al. used Tung's theoretical approach and found a linear correlation between the experimental Φ_{bo} and n [8,23].

A plot of the experimental Φ_{bo} vs n for an Au/n-CdTe Schottky solar cell at the temperature range 120–380 K is shown in Fig. 4. Here, a linear relationship between Φ_{bo} and n is found, which was explained by the lateral inhomogeneities of the BHs in the structure. The value of correlation coefficient or R^2 of Φ_{bo} vs n plot is 0.9499 in the whole temperature range and except for the first data (120 K) is 0.982. We think this value of R^2 is enough for an evidence for a linear fit. Thus, the extrapolation of the experimental Φ_{bo} vs n plot to $n=1$ yields a homogeneous BH of approximately 0.896 eV. Thus, the significant decrease in the

zero-bias BH and increase in the ideality factor, especially at low temperatures, are possibly caused by the BH inhomogeneties.

To explain the commonly observed abnormal deviation from the classical TE theory, some researchers have successfully explained the phenomenon based on a TE with GD of BHs due to the BH inhomogeneities prevailing at the M/S interface [21–27]. The Gaussian function can be expressed by the following relation:

$$P(\Phi_b) = \frac{1}{\sigma_s\sqrt{2\pi}}\exp\left[-\frac{(\Phi_b-\overline{\Phi}_{bo})^2}{2\sigma_s^2}\right], \tag{5}$$

where $1/\sigma_s\sqrt{2\pi}$ corresponds to the normalization constant of the GD of the BH distribution. The total current $I(V)$ through the barrier for the forward bias can be expressed as

$$I(V) = \int_{-\infty}^{+\infty} I(\Phi_b,V)P(\Phi_b)d\Phi, \tag{6}$$

where $I(\Phi_b, V)$ is the current at a bias V for a barrier of height based on the ideal Thermionic-emission–diffusion theory, and $P(\Phi_b)$ is the normalized distribution function yielding the probability of accuracy for BH. Now, substituting $I(\Phi_b, V)$ and $P(\Phi_b)$ from Eqs. (1) and (5) into Eq. (6), and carrying out this integration from $-\infty$ to $+\infty$, one can obtain the current $I(V)$ through an SB, similar to Eqs. (1) and (2) but with the modified barrier, as follows:

$$I(V) = AA^*T^2\exp\left[-\frac{q}{kT}\left(\overline{\Phi}_{ap}-\frac{q\sigma_s^2}{2kT}\right)\right]\exp\left(\frac{qV}{n_{ap}kT}\right)\left[1-\exp\left(-\frac{qV}{kT}\right)\right] \tag{7}$$

with

$$I_o = A\ A^*\ T^2\ \exp\ \left(-\frac{q\Phi_{ap}}{kT}\right), \tag{8}$$

where $\overline{\Phi}_{ap}$ and n_{ap} are the apparent zero-bias BH and the apparent ideality factor, respectively, and are derived using the following expressions [13,21–24]:

$$\Phi_{ap} = \overline{\Phi}_{bo}(T=0)-\frac{q\sigma_s^2}{2kT}; \tag{9}$$

$$\left(\frac{1}{n_{ap}}-1\right) = \rho_2-\frac{q\rho_3}{2kT}. \tag{10}$$

It is assumed that the mean BH $\bar{\phi}_b$ and σ_{s} are linearly bias dependent on the Gaussian parameters such as $\phi_b = \phi_{bo} + \rho_2 V$ and $\sigma_s = \sigma_{so} + \rho_3 V$, where ρ_2 and ρ_3 are the voltage coefficients that may depend on temperature, and they quantify the voltage deformation of the BH distribution [17–20]. Here, the temperature dependence of σ_{so} is usually small and can be neglected. A plot of Φ_{ap} vs $q/2kT$ (as in Fig. 5) has been drawn to obtain evidence of the GD of the BHs, and values of Φ_{bo} and σ_s were obtained from this plot as 1.023 eV and 0.12 V, respectively. Moreover, as can be observed in the same figure (Fig. 5), the plot of $(1/n_{ap} - 1)$ vs $q/2kT$ shows a linear behavior that yields the voltage coefficients ρ_2 and ρ_3 from the intercept and slope, respectively. The values of ρ_2 and ρ_3 were obtained from this plot as -0.1138 V and -0.012 V, respectively.

Now, combining Eqs. (7) and (9), the following expression is obtained:

$$\ln\left(\frac{I_0}{T^2}\right) - \left(\frac{q^2\sigma_o^2}{2k^2T^2}\right) = \ln(AA^*) - \frac{q\bar{\Phi}_{b0}}{kT}. \tag{11}$$

It can be seen that the modified activation energy plot (Fig. 6) has a relatively good linearity over the entire temperature range with the slope directly yielding the mean $\bar{\Phi}_{b0}$ as 1.029 eV and the
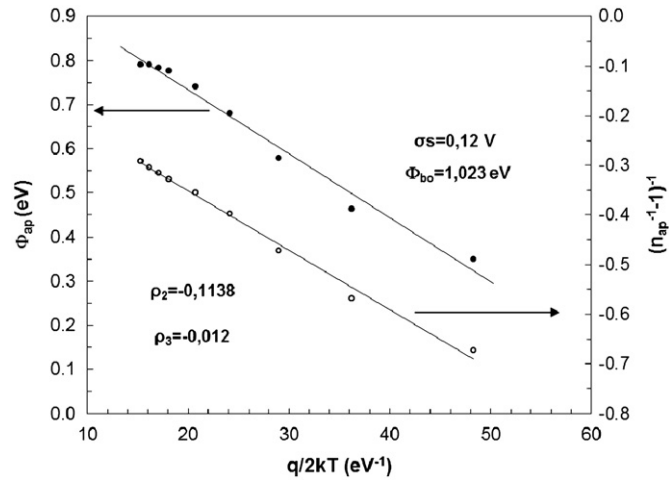

Fig. 5. Zero-bias apparent barrier height Φ_{ap} (the filled circles) vs $q/2kT$ and $(n_{ap} - 1)^{-1}$ vs $q/2kT$ curves of the Au/n-CdTe schottky solar cell according to the two Gaussian distributions of BHs.
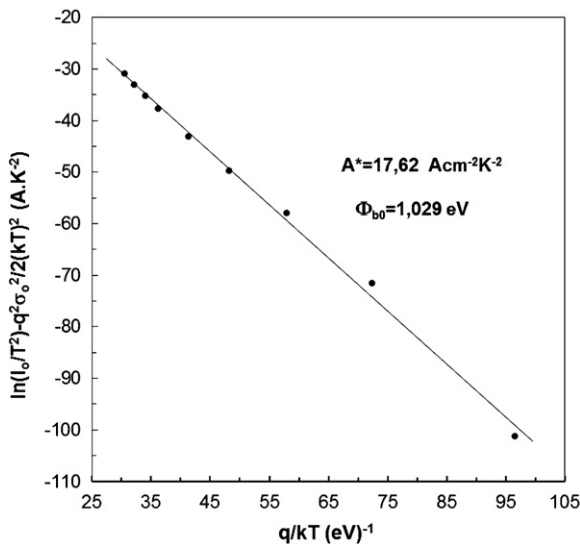

Fig. 6. Modified Richardson $\ln(I_0/T^2) - q^2\sigma_0^2/2(kT)^2$ vs q/kT plot for the Au/n-CdTe Schottky solar cell according to the GD of BHs.

intercept at the ordinate determining A^* for a given Schottky solar cell area as 17.62 A cm^{-2} K^{-2}, without using the temperature coefficient of the BHs. This value of $A^* = 17.62$ A cm^{-2} K^{-2} is close to the theoretical value of 12 A cm^{-2} K^{-2} for n-CdTe [2].

In addition, the experimental C–V and C^{-2}–V plots at 1 MHz for Au/n-CdTe Schottky solar cell are shown in Fig. 7 at room temperature. The charges at the interface states cannot follow an ac signal when the measurements are carried out at high frequency ($f \geq 1$ MHz) [16,28]. Therefore, the C–V measurements were conducted at 1 MHz. When a small ac voltage of a few mV is applied to a reverse-biased diode, the depletion-region capacitance C is provided by the relation,

$$C^{-2} = \frac{2}{q\varepsilon_s A^2 N_d}(V_o + V), \tag{12}$$

where A is the area of the solar cell, ε_s is the permittivity of semiconductor, N_d is the carrier-doping density of donors, V is the magnitude of the applied bias, and V_0 is the intercept of C^{-2} with the voltage axis and is given by

$$V_0 = V_D + kT/q \tag{13}$$

We have drawn C^{-2} vs V plot at 1 MHz to determine the doping concentration (N_d) and BH at room temperature and compare the mean value of BH obtained from the forward bias I–V data. The nature of forward bias I–V and reverse bias C–V measurements are different and non-ideal behavior emerges only in forward bias I–V measurements. Therefore, the C–V measurements are not carried out in the wide temperature range. As shown in Fig. 7, the C^{-2}–V plots at 1 MHz gives straight lines at the wide-bias voltage region. Thus, the value of the barrier was obtained from Fig. 7 as follows [16,28]:

$$\Phi_b(C-V) = V_o + kT/q + E_F = V_D + E_F. \tag{14}$$

The value of $\Phi_b(C-V)$ was determined from the C^{-2} vs V plot as 1.32 eV. It is clear that this value of $\Phi_b(C-V)$ is higher than the value of Φ_{bo} ($= 0.78$ eV) determined from the forward-bias I–V measurements at room temperature. This discrepancy between the values of $\Phi_{bo}(I-V)$ and $\Phi_b(C-V)$ may be due to the existence of excess capacitance in the structure due to the interface states or presence barrier inhomogeneities [26,28]. This value of Φ_{bo} is relevant at room temperature. However, the mean value of BH obtained from Figs. 5 and 6 is 1.023 eV. It is clear that there is a discrepancy of BH obtained from reverse bias C–V plot and forward bias I–V plot is 0.291 eV. In recent year, similar results have been reported in the literature [29–32]. On the other hand, the nature of forward and
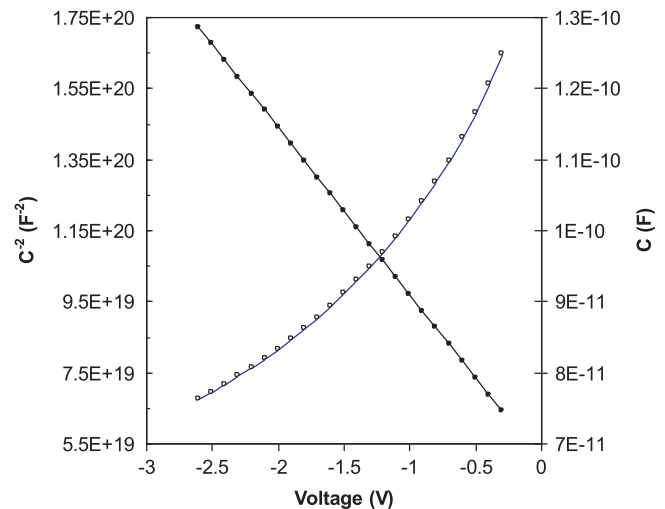

Fig. 7. The plots of forward and reverse bias C vs V and C^{-2} vs V of the Au/n-CdTe Schottky solar cell at room temperatures.

reverse bias is different and the value of BH obtained reverse bias C–V data is always higher than the obtained one from forward bias as the Fermi energy level [29] due to the nature of measurement system, the existence of excess capacitance in the structure due to the interface states, interfacial insulator layer and the voltage dependent of BH.

4. Conclusion

The current-conduction/transport mechanisms in the Au/n-CdTe Schottky solar cells have been investigated in the temperature range 120–380 K. The analysis of the forward bias I–V characteristics based on the TE theory showed an abnormal increase in Φ_{bo} and a decrease in n with the increasing temperature, which leads to nonlinearity in the conventional activation energy plot of $\ln(I_0/T^2)$ vs $1/T$. Furthermore, this temperature dependence of Φ_{bo} is an obvious disagreement with the reported negative temperature coefficient of the E_g or BH. Such behavior of Φ_{bo} and n is attributed to the SB inhomogeneities and is explained by assuming a GD of BHs due to the barrier inhomogeneities that prevail at Au/n-CdTe interface. In order to obtain the evidence of a GD of the BHs, a plot of Φ_{bo} vs $q/2kT$ has been drawn, and the values of $\overline{\Phi}_{bo}$ and σ_s were found this plot as 1.023 eV and 0.12 V, respectively. Thus, in the modified $(\ln(I_0/T^2) - q^2\sigma_s^2/2k^2T^2)$ vs q/kT plot, the values of Φ_{bo} and A^* were obtained as 1.029 eV and 17.62 A cm^{-2} K^{-2}, respectively. The value of $A^* = 17.62$ A cm^{-2} K^{-2} is close to the known value of 12 A cm^{-2} K^{-2} for electrons in n-type CdTe. Therefore, it has been concluded that the temperature dependence of the forward-bias I–V characteristics of the Au/n-CdTe Schottky solar cell can be successfully explained based on the TE mechanism with a GD of BHs. In addition, the value of $\Phi_b(C$–$V)$ is greater than the value of $\Phi_{bo}(I$–$V)$ obtained at room temperature. This discrepancy between these can be attributed to the nature of measurement system, the existence of excess capacitance in the structure due to the interface states, interfacial insulator layer and the voltage dependent of BH.

References

[1] J.P. Ponpon, P. Siffert, Rev. Phys. Appl. (Paris) 12 (1977) 427.
[2] D. Donoval, M. Barus, M. Zdimal, Solid State Electron. 34 (1991) 1365.
[3] M. Pattabi, S. Krishnan, Ganesh, X. Mathew, Sol. Energy 81 (2007) 111.
[4] X. Mathew, P.J. Sebastian, A. Sanchez, J. Campos, Sol. Energy Mater. Sol. Cells, 59 (1999) 99.
[5] X. Mathew, Semicond. Sci. Technol. 18 (2003) 1–6.
[6] S. Chand, J. Kumar, Semicond. Sci. Technol. 10 (1995) 1680.
[7] I.M. Dharmadasa, G.G. Roberts, M.C. Petty, J. Phys. D: Appl. Phys. 15 (1982) 901.
[8] R.T. Tung, Mater. Sci. Eng. R 35 (2001) 1.
[9] J.H. Werner, H.H. Güttler, J. Appl. Phys. 69 (1991) 1522.
[10] Y.P. Song, R.L. Van Meirhaeghe, W.H. Laflere, F. Cardon, Solid State Electron. 29 (6) (1986) 663.
[11] S. Chand, J. Kumar, J. Appl. Phys. 82 (10) (1997) 5005.
[12] J.P. Sullivan, R.T. Tung, M.R. Pinto, W.R. Graham, J. Appl. Phys. 70 (1991) 7403.
[13] S. Chand, J. Kumar, Semicond. Sci. Technol. 12 (1997) 899.
[14] E. Dobrocka, J. Osvald, Appl. Phys. Lett. 65 (1994) 575.
[15] M.K. Hudait, P. Venkateswarlu, S.B. Krupanidhi, Solid State Electron. 45 (2001) 133.
[16] S.M. Sze, Physics Semiconductor Devices, John Wiley & Sons, New York, 1981.
[17] S. Chand, S. Bala, Physica B 390 (2007) 179.
[18] W. Mönch, J. Vac. Sci. Technol. B 17 (1999) 1867.
[19] A. Gümüş, A. Türüt, N. Yalçın, J. Appl. Phys. 91 (2002) 245.
[20] R.T. Tung, Appl. Phys. Lett. 58 (1991) 2821.
[21] S. Karatas, S. Altındal, A. Turut, A. Ozmen, Appl. Surf. Sci. 217 (2003) 250.
[22] S. Altındal, H. Kanbur, D.E. Yıldız, M. Parlak, Appl. Surf. Sci. 253 (2007) 5056.
[23] R.F. Schmitsdorf, R.T. Tung, M.R. Pinto, J. Appl. Phys. 70 (1991) 7403.
[24] E. Arslan, Ş. Altındal, S. Özçelik, E. Ozbay, J. Appl. Phys. 105 (2009) 023705.
[25] S. Hardikar, M.K. Hudait, P. Modak, S. Krupanidhi, N. Padha, Appl. Phys. A 68 (1999) 49.
[26] A.F. Özdemir, A. Türüt, A. Kökçe, Semicond. Sci. Technol. 21 (2006) 298.
[27] S. Zeyrek, Ş. Altındal, H. Yüzer, M.M. Bülbül, Appl. Surf. Sci. 252 (2006) 2999.
[28] E.H. Rhoderick, R.H. Williams, Metal Semiconductor Contacts, 2nd ed., Clarendon Press, Oxford, 1988.
[29] K. Ejderha, N. Yıldırım, B. Abay, A. Turut, J. Alloys Compd. 484 (2009) 870.
[30] A. Tataroğlu, Ş. Altındal, J. Alloys Compd. 484 (2009) 405.
[31] M. Soylu, F. Yakuphanoglu, J. Alloys Compd. 2011 (2010) 418.
[32] K. Ejderha, N. Yıldırım, A. Turut, B. Abay, Superlatice Microstruct. 47 (2010) 241.